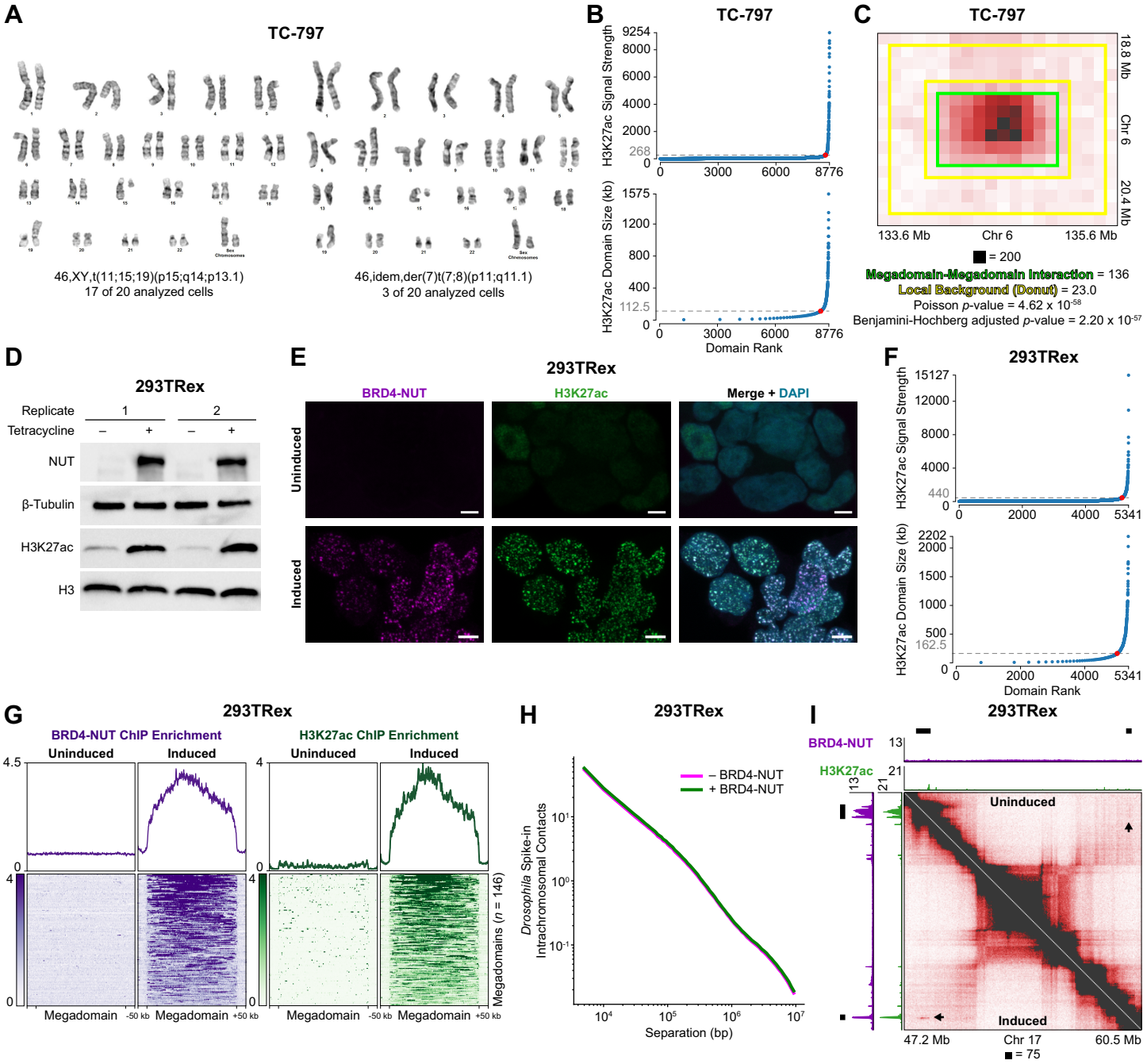

Figure S1. Characterization of TC-797 cells and Megadomain-Megadomain Interactions in 293TRex Cells, Related to Figure 1

(A) Representative Giemsa banding analysis of TC-797 cells confirming that all analyzed cells contain the reported t(11;15;19)(p15;q14;p13.1) rearrangement (Toretsky et al., 2003) resulting in the BRD4-NUT fusion.

(B) Input-normalized ChIP-seq signal strength (left) and domain size (right) of rank ordered SICER/epic-identified histone H3K27ac domains in TC-797 cells. The subset of domains with an exceptionally high amount of histone H3K27ac or that are exceptionally large are indicated above the dashed gray line and open red circle. The intersection of these domains was used to identify megadomains in TC-797 cells.

(C) Schematic of regions used for determining significant megadomain-megadomain interactions. The green region is the megadomain-megadomain interaction region determined by the intersection of two

distinct megadomains identified by ChIP-seq; the yellow region is the donut local background region. Values below the contact map represent those used for, and the results of, statistical significance testing and multiple hypothesis correction.
(D) Western blot analysis of 293TRex Flp-In cells containing inducible Flag-BRD4-NUT-HA at a FRT site confirms expression of BRD4-NUT after treatment with tetracycline.
(E) Immunofluorescence for BRD4-NUT (magenta) and histone H3K27ac (green) from uninduced and induced 293TRex cells expressing BRD4-NUT counterstained with DAPI (blue) indicates nuclear foci formation after induction of BRD4-NUT. Scale bars, 5 μm.
(F) Input-normalized ChIP-seq signal strength (left) and domain size (right) of rank ordered SICER/epic-identified histone H3K27ac domains in 293TRex cells. The subset of domains with an exceptionally high amount of histone H3K27ac or that are exceptionally large are indicated above the dashed gray line and open red circle. The intersection of these domains was used to identify megadomains in 293TRex cells.
(G) Mean BRD4-NUT (purple) and histone H3K27ac (green) ChIP-seq profiles for megadomains (upper) and heatmap of the ChIP-seq signal for each megadomain (lower) from uninduced and induced 293TRex cells expressing BRD4-NUT demonstrating megadomain formation due to BRD4-NUT expression. Megadomains were normalized to the same length and 50 kb of flanking DNA is shown next to each normalized megadomain.
(H) Average intrachromosomal contacts for loci from identical amounts of Kc167 *Drosophila melanogaster* cultured cells spiked-in to identical amounts of uninduced (magenta) and induced (green) 293TRex cells expressing BRD4-NUT separated by the distance given on the abscissa. Overlap of *Drosophila* spike-in data from the uninduced and induced conditions at all genomic separations indicates no technical differences in Hi-C analysis between the uninduced and induced human samples (Paul et al., 2018).
(I) Hi-C contact map at 50 kb resolution of uninduced (above the diagonal) and induced (below the diagonal) 293TRex cells expressing BRD4-NUT. BRD4-NUT (magenta) and histone H3K27ac (green) ChIP-seq profiles are aligned with the maps. Black bars indicate megadomains identified in induced cells. Arrows indicate a megadomain-megadomain interaction in the induced, but not the uninduced cells. Maximum Hi-C contact intensity is indicated by the black box beneath each map.

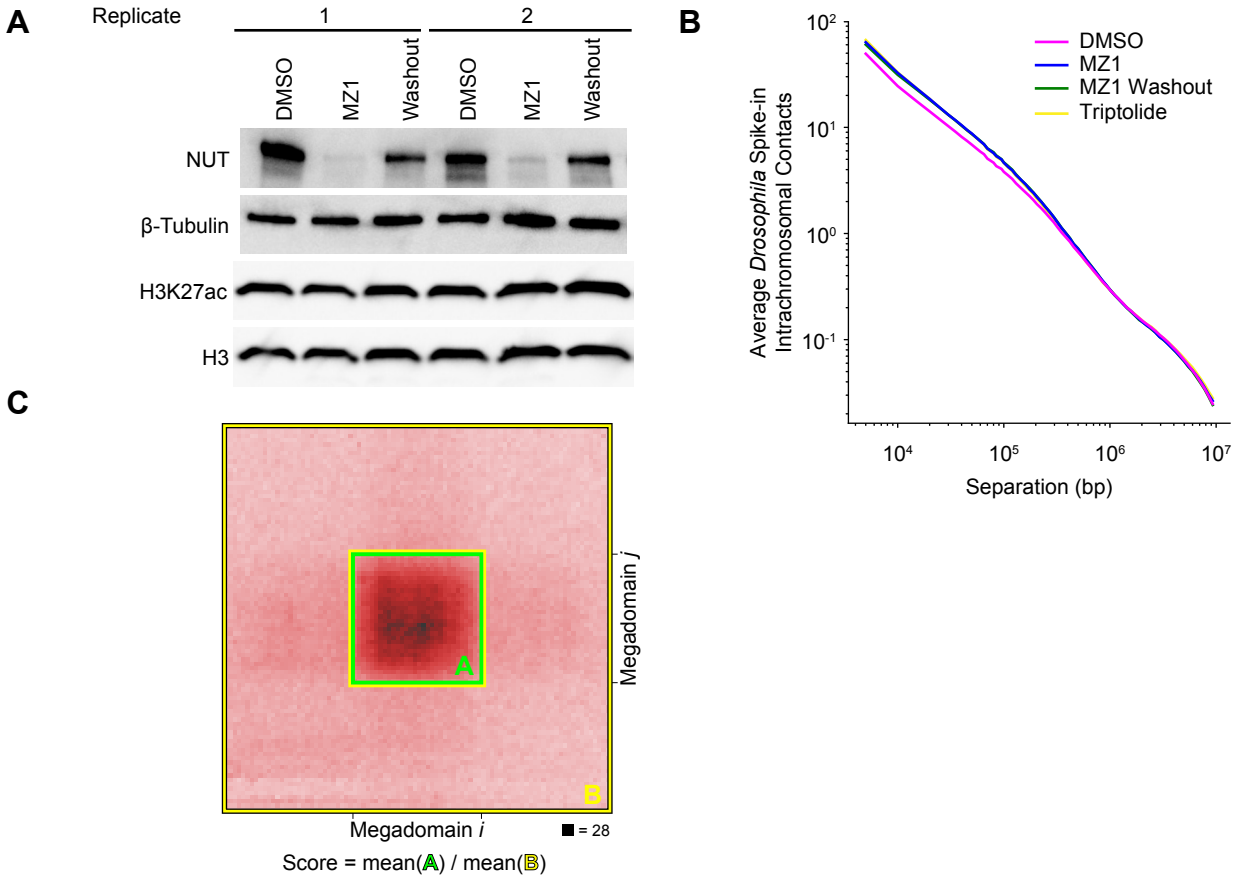

Figure S2. MZ1 Treatment and Washout of TC-797 cells, Related to Figure 2

(A) Western blot analysis of TC-797 cells treated with DMSO, MZ1 (4 hours), or MZ1 followed by drug washout (24 hours) confirms essentially complete removal of BRD4-NUT by MZ1 that recovered after drug washout, but no change in histone H3K27ac levels.

(B) Average intrachromosomal contacts for loci from identical amounts of Kc167 *Drosophila melanogaster* cultured cells spiked-in to identical amounts of TC-797 cells treated with DMSO, MZ1, MZ1 followed by drug washout, or triptolide separated by the distance given on the abscissa. Overlap of *Drosophila* spike-in data from the DMSO, MZ1, MZ1 followed by drug washout or triptolide conditions at loci separated by ≥ 1 Mb separations, which is the minimum distance between interacting megadomains in DMSO treated TC-797 cells, indicates no technical differences in Hi-C analysis between the human samples (Paul et al., 2018). For aggregate domain analysis (ADA), the human samples were normalized to the DMSO sample based on the *Drosophila* spike-in data to account for slight differences in expected contact frequency for loci separated by < 1 Mb.

(C) Schematic of regions used for determining the domain-domain interaction score for megadomain-megadomain interactions. Region A (green) is the re-scaled (by linear interpolation and block averaging) megadomain-megadomain interaction region; region B (yellow) is the region excluding the megadomain-megadomain interaction region. The domain-domain interaction score is the ratio of the mean of the values in region A to the mean of the values in region B, with a value of 1 indicating no enrichment in interactions relative to local background.

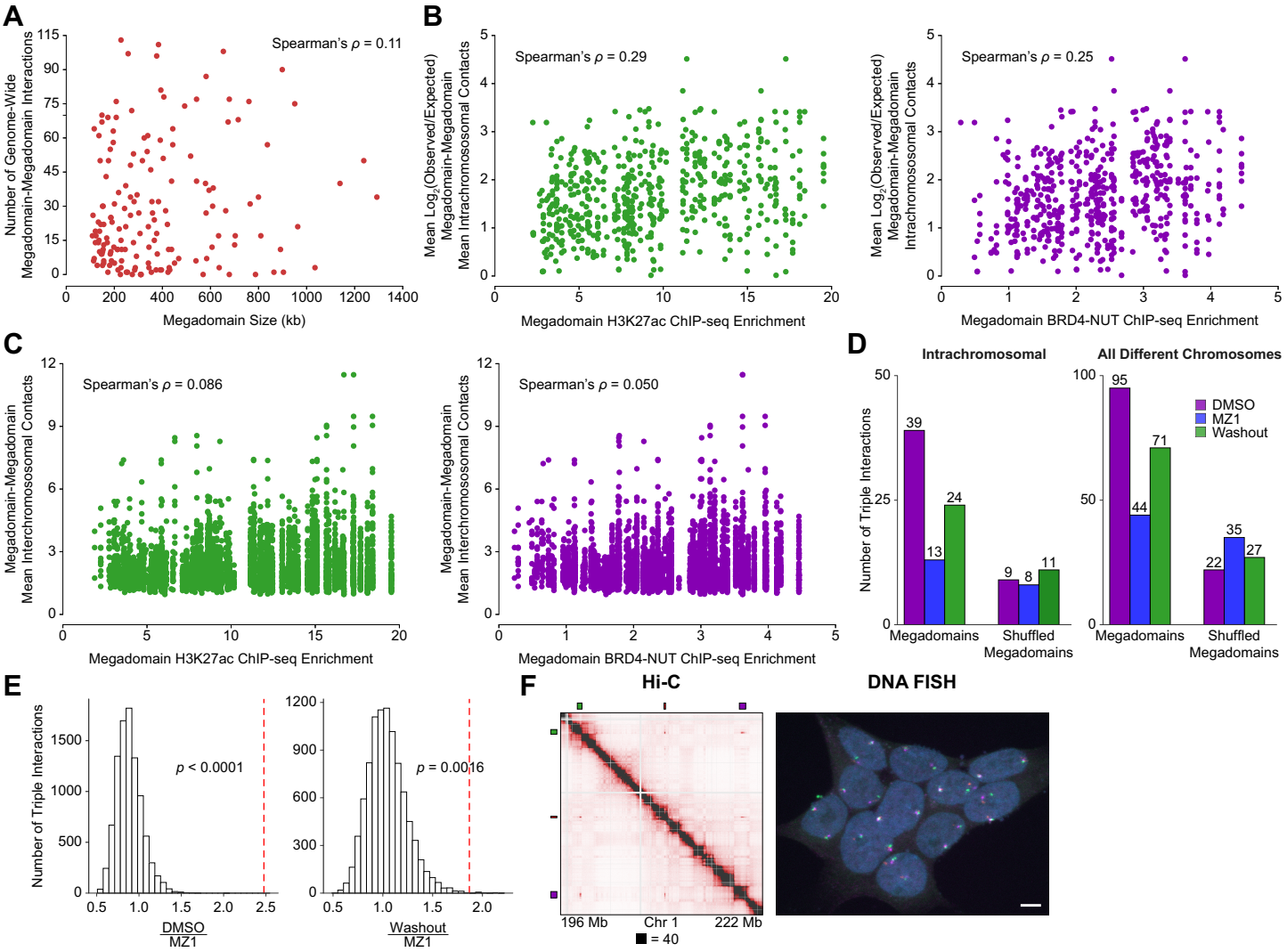

Figure S3. Further Characterization of Pairwise and Triple Megadomain-Meagadomain Interactions, Related to Figure 3

(A) For each megadomain, the number of genome-wide (intra- and interchromosomal) megadomain-megadomain interactions versus megadomain size indicates no correlation between megadomain size and number of megadomain-megadomain interactions.

(B) For each megadomain, the mean number of $\log_2$(observed/expected) megadomain-megadomain intrachromosomal contacts for each interacting megadomain-megadomain pair versus the average histone H3K27ac (green) or BRD4-NUT (purple) ChIP-seq enrichment within that megadomain indicates no correleation between histone H3K27ac and BRD4-NUT ChIP-seq enrichments and pairwise intrachromosomal megadomain-megadomain interaction strength. ChIP-seq enrichment was normalized for differences in megadomain size.

(C) For each megadomain, the mean number of megadomain-megadomain interchromosomal contacts for each interacting megadomain-megadomain pair versus the average histone H3K27ac (green) or BRD4-NUT (purple) ChIP-seq enrichment within that megadomain indicates no correleation between histone H3K27ac and BRD4-NUT ChIP-seq enrichments and pairwise interchromosomal megadomain-megadomain interaction strength. ChIP-seq enrichment was normalized for differences in megadomain size.

(D) Normalized counts of triple interactions between three distinct megadomains each located on the same chromosome (left) or each located on different chromosomes (right) in TC-797 cells treated with

DMSO, MZ1, or MZ1 followed by drug washout demonstrating reduction in triple interactions after MZ1 treatment that partially recovered after drug washout for both intra-chromosomal and inter-chromosomal interactions. The observed megadomain triple interactions are compared to a random shuffled control set of interactions.
(E) Histogram of 10,000 random shuffle triple interactions between DMSO treated versus MZ1 treated (left) and MZ1 treated followed by drug washout (right) TC-797 cells. *P*-values were then determined by comparing the observed ratio to the distribution of shuffled ratios using a random permutation test indicating that the chance of observed enrichment of triple interactions is DMSO and drug washout treated cells compared to MZ1 treated cells is less than 0.0001 and 0.0016, respectively.
(F) Hi-C contact map (left) at 25 kb resolution for TC-797 cells. Bars indicate megadomains and colors represent probes for DNA FISH (right), which demonstrate megadomain clustering. Scale bars, 5 μm.

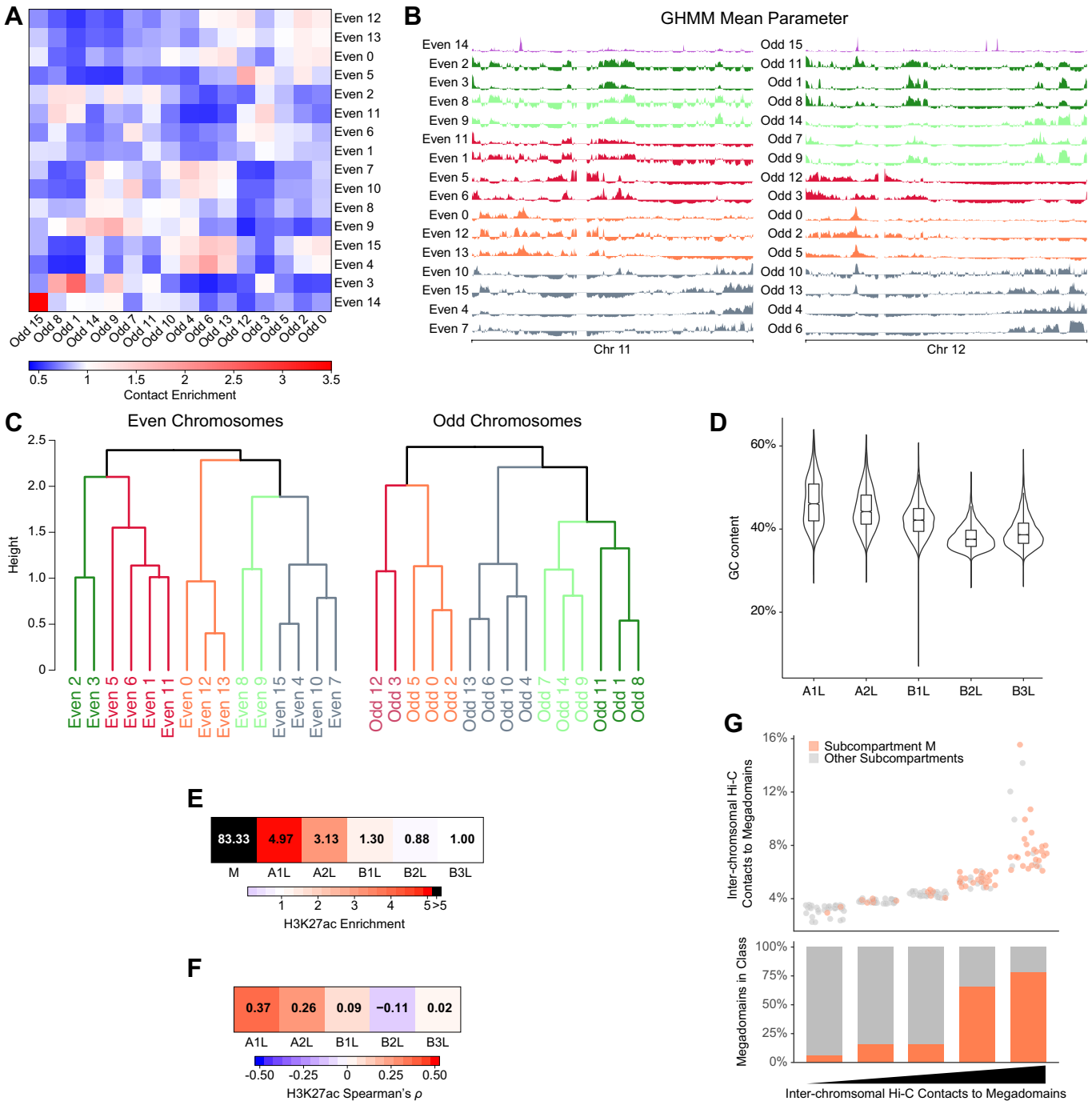

Figure S4. Subcompartment Annotation in TC-797 cells, Related to Figure 3

(A) Contact enrichment between 16 states identified independently from the even and odd chromosomes by a Gaussian hidden Markov model (GHMM).

(B) The mean parameter estimated by the GHMM applied independently to the even and odd chromosomes. Tracks were colored according to the merged states (see Materials and Methods for details).

(C) Hierarchical clustering dendrogram of contact enrichment matrix from (A) after removing the even 14 and odd 15 states. This clustering was used to merge states with similar patterns of contact enrichment that may have been inadvertently split during GHMM clustering.

(D) GC content, calculated in 100 kb bins, for each subcompartment. GC content is indicated by violin plots that are overlaid with notched box plots with the median GC content indicated as a horizontal line. Black dots are outliers.
(E) Histone H3K27ac enrichment in subcompartments. Histone H3K27ac enrichment was determined by taking the median value of the H3K27ac ChIP-seq profile in each 100 kb bin within the subcompartment of interest and dividing in by the genome-wide median value the H3K27ac ChIP-seq profile across all bins.
(F) Spearman's correlation coefficient (ρ) between the H3K27ac ChIP-seq profile (100 kb bins) and a pseudo track for each subcompartment. The pseudo track was defined to have a value of 1 at each 100 kb bin that belonged to a subcompartment of interest and a value of 0 elsewhere. Subcompartment M was not considered because this subcompartment was too small to generate a meaningful genome-wide pseudo track.
(G) The mean number of inter-chromosomal Hi-C contacts to megadomains in 100 kb bins was aggregated for each megadomain, ranked, and then split into five equally sized groups. Orange dots represent 35% of megadomains (58 of 164) that are within subcompartment M; gray dots represent megadomains outside of subcompartment M. The bar plot indicates the proportion of megadomains within (orange) or outside of (gray) subcompartment M for each quintile. Those megadomains not in subcompartment M either don't make detectable inter-chromosomal interactions with other megadomains or these interactions are not strong enough to be detected by the Gaussian hidden Markov model.

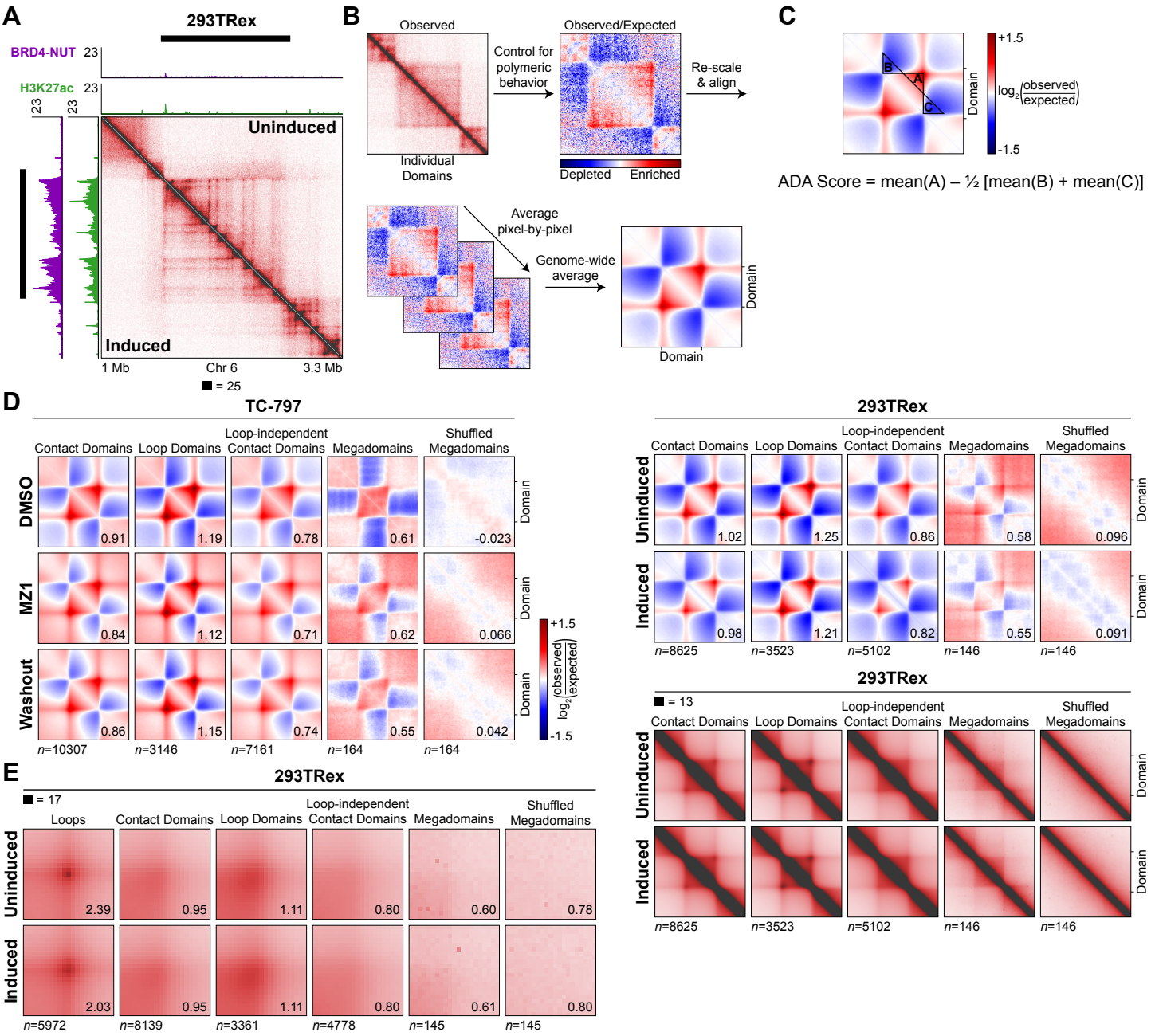

Figure S5. Local Chromatin Organization is Unchanged After Induction of BRD4-NUT, Related to Figure 4

(A) Hi-C contact maps at 5 kb resolution of uninduced (above the diagonal) and induced (below the diagonal) 293TRex cells expressing BRD4-NUT. BRD4-NUT (magenta) and histone H3K27ac (green) ChIP-seq profiles are aligned with the maps. Black bars indicate megadomains identified in induced 293TRex cells.

(B) Schematic of genome-wide, aggregate domain analysis (ADA). First, each domain plus flanking DNA is extracted from the observed Hi-C contact map. Next, to control for the polymeric nature of chromosomes (Lieberman-Aiden et al., 2009), that is loci separated by small linear distances more likely to be in close spatial proximity than loci separated by large linear distances, we applied a correction for this polymeric behavior. This correction divides the observed number of contacts between two loci by the number of expected interactions based on polymeric fluctuations in the chromatin fiber. Such a correction ensures that smaller domains, which have more intense Hi-C signals than larger

domains, particularly at their corners, do not overly bias the average signal in subsequent steps after all domains have been re-scaled to the same size. This so-called observed/expected correction also highlights contacts that occur more or less often than those due to unorganized chromosome folding. Finally, all regions are re-scaled to the same dimensions and then the observed/expected signal is averaged, pixel-by-pixel, across all regions. Since chromosomes are organized into self-associating contact domains, the example domain shown here demonstrates characteristics of all contact domains: both a characteristic enrichment of contacts within the contact domain and a characteristic depletion of contacts at contact domain boundaries.

(C) Schematic of regions used for determining the ADA score, which quantitatively assesses domain structure from the observed/expected ADA matrix. The ADA score measures the difference between the mean number of observed/expected contacts within domains to those at domain boundaries, with an ADA score of 0 indicating no difference in domain interior versus domain boundary contacts. Region A is within the domain, immediately adjacent to the domain corner; regions B and C are at the domain boundaries. The ADA score is the difference of the mean of the values in region A and ½ the sum of the mean of the values in region B and the mean of the values in region C.

(D) Genome-wide, aggregate domain analysis (ADA) at 5 kb resolution of Hi-C signal from uninduced and induced 293TRex cells expressing BRD4-NUT (left) and from DMSO, MZ1, and MZ1 followed by drug washout treated TC-797 cells (right) for contact domains, loop domains, loop-independent contact domains, megadomains, and random shuffled control megadomains. The ADA score for observed megadomains and contact domains was essentially unchanged after induction of BRD4-NUT in 293TRex cells (left) or after treatment of TC-797 cells with MZ1 (right). After dividing contact domains into loop domains (contact domains that have a loop at their corner) and loop-independent contact domains (contact domains that do not have a loop at their corner), ADA plots and ADA scores for megadomains more closely resembled that for loop-independent contact domains than loop domains. Megadomains were more similar to loop-independent contact domains than a random shuffled control set of megadomains. ADA scores for randomly shuffled control sets of megadomains were essentially 0. Contact domain annotations are from uninduced or DMSO treated 293TRex and TC-797 cells, respectively; megadomain locations from induced or DMSO treated 293TRex and TC-797 cells, respectively. ADA scores are given at bottom right. The bottom two rows for 293TRex cells is similar to the top two rows, except observed, rather than observed/expected data are shown; this is also the same analysis as Figure 4B for TC-797 cells.

(E) Genome-wide, aggregate peak analysis (APA) at 5 kb resolution of Hi-C signal from uninduced and induced 293TRex cells expressing BRD4-NUT centered on loops, contact domain corners, megadomain corners, and random shuffled control megadomain corners. For APA, each single pixel of interest (e.g. peak pixel of a chromatin loop) plus a constant amount of flanking DNA (50 kb) is extracted from the Hi-C contact map and then all extracted regions are averaged. Along with APA plots, APA scores quantitatively assess the enrichment of the central pixel to the average signal in the lower-left quadrant of APA plots, with a value above 1 indicating a relative enrichment of the central pixel (Rao et al., 2014). Since chromatin loops exhibit radially symmetric focal peaks of contact enrichment, they characteristically have a robust, centrally enriched APA signal and APA score greater than 1 (Rao et al., 2014). APA analysis of the corners of megadomains did not exhibit this characteristic APA signal. Furthermore, the APA score for megadomain and contact domain corners was less than 1, consistent with an observed weak enrichment of signal in the lower-left quadrant of APA plots for both megadomains and contact domains. Since APA analysis focuses on contacts above the diagonal,

the lower-left quadrant represents the interior of domains and a weak signal within this quadrant reflects enrichment of intra-domain contacts, which is characteristic of contact domains. There was no enrichment within this quadrant for a randomly shuffled control set of megadomains. After dividing contact domains into loop domains (contact domains that have a loop at their corner) and loop-independent contact domains (contact domains that do not have a loop at their corner), APA plots and scores for megadomains was also more similar to the APA plots and scores for the corners of loop-independent contact domains than those for the corners of loop domains. Loop and contact domain annotations and megadomain locations are from uninduced 293TRex cells. APA scores are given at bottom right.

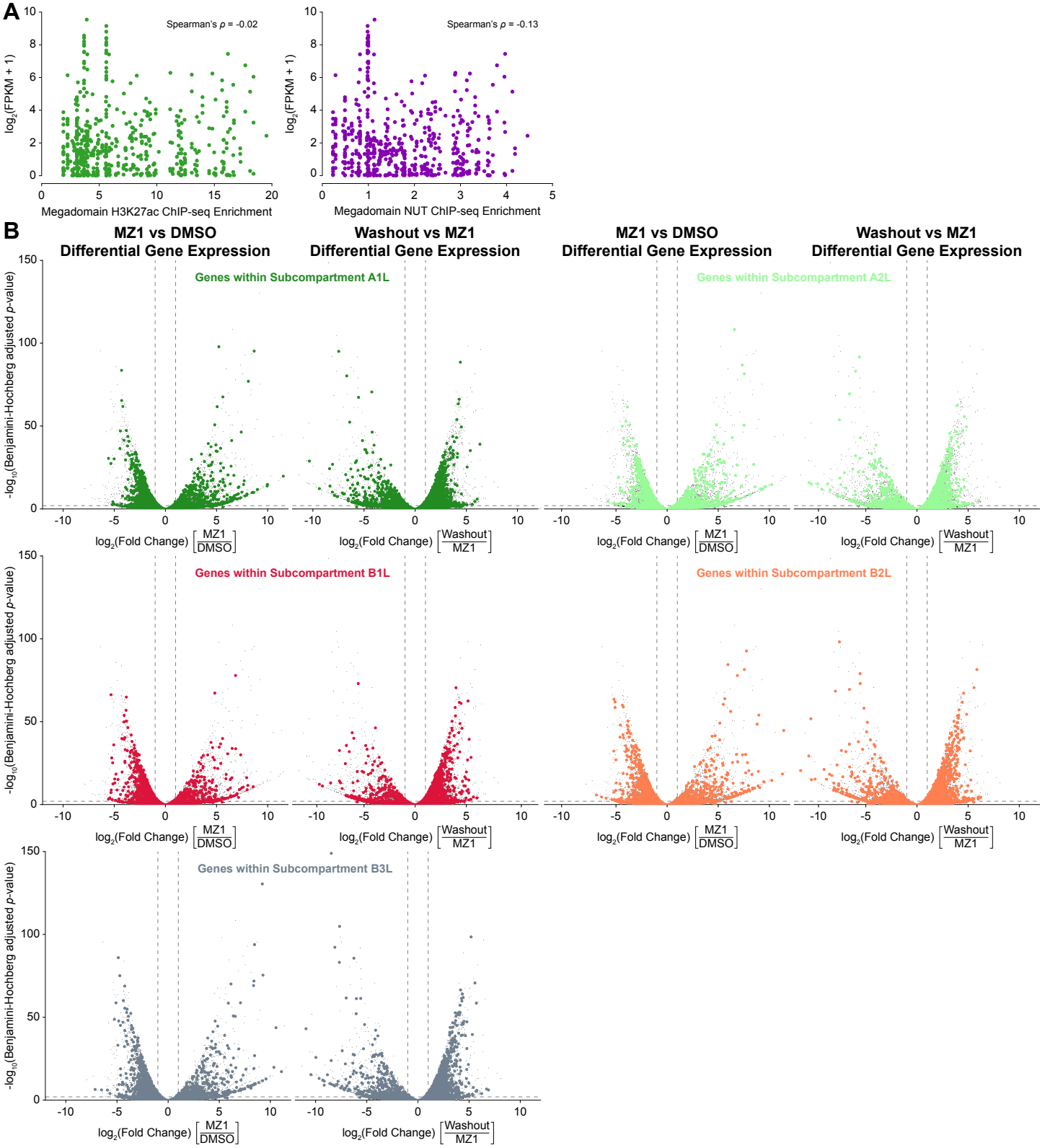

Figure S6. Genes Within Subcompartments Other Than Subcompartment M Are Neither Specifically Downregulated Nor Specifically Upregulated After MZ1 Treatment, Related To Figure 6

(A) For genes within megadomains, expression level versus the average histone H3K27ac (green) or BRD4-NUT (purple) ChIP-seq enrichment within the megadomain containing the gene.

(B) Volcano plots (significance versus fold change) of differentially expressed genes show that after MZ1 treatment genes within subcompartments other than subcompartment M are neither specifically

downregulated (left) nor specifically upregulated (right) in TC-797 cells. Horizontal dashed line indicates a Benjamini-Hochberg adjusted *p*-value of 0.01; vertical dashed lines indicate 2-fold change in expression.

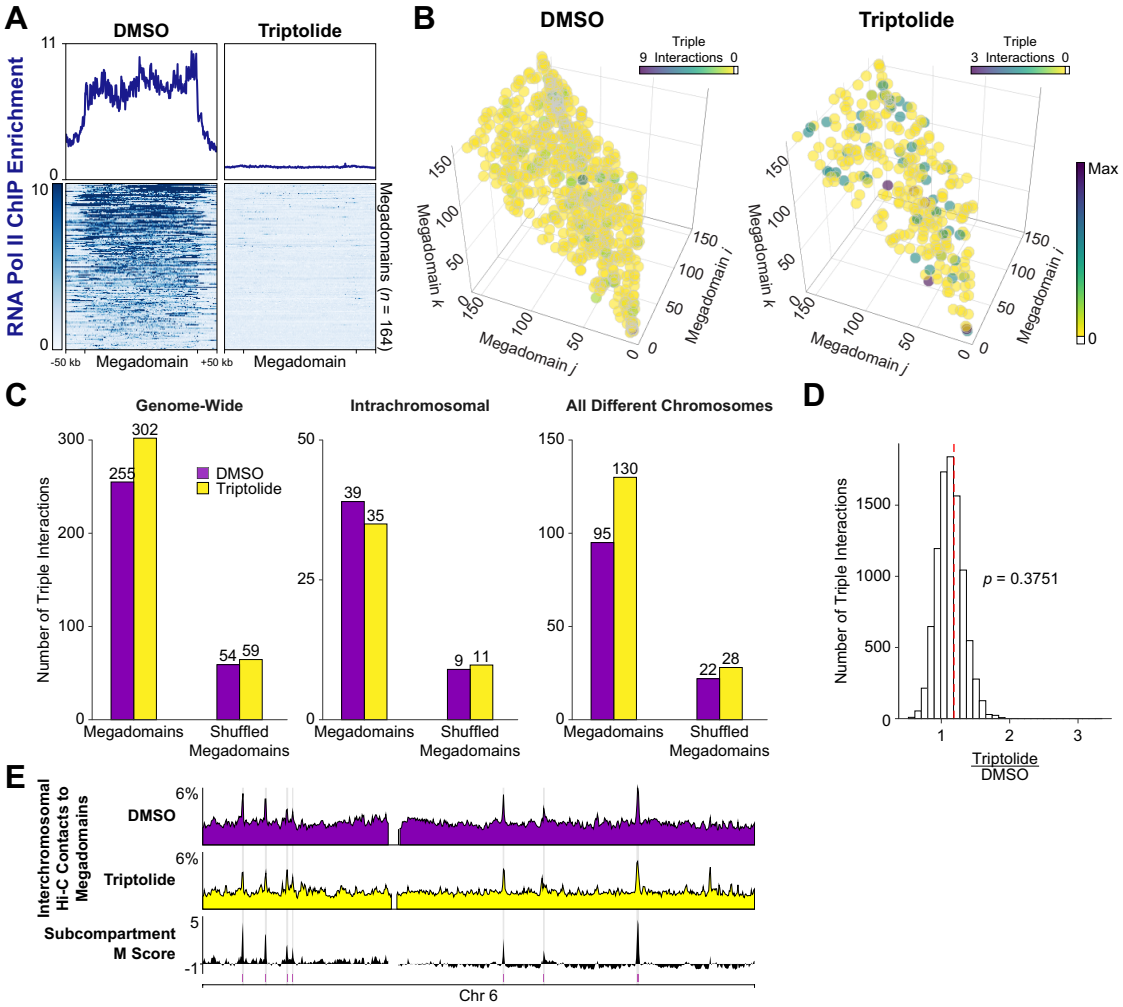

Figure S7. Triple Megadomain Interactions and Subcompartment M Persist In The Absence Of Transcription, Related To Figure 7

(A) Mean RNA polymerase II ChIP-seq profiles for megadomains (upper) and heatmap of the ChIP-seq signal for each megadomain (lower) from TC-797 cells treated with DMSO or triptolide indicates clearance of RNA polymerase II from megadomains after triptolide treatment.

(B) Three-dimensional plot of triple interactions between different megadomains in TC-797 cells treated with DMSO or triptolide. The coordinate along each axis represents a distinct megadomain.

(C) Normalized counts of triple interactions between three distinct megadomains genome-wide (left), each located on the same chromosome (middle), or each located on different chromosomes (right) in TC-797 cells treated with DMSO or triptolide demonstrating no difference in the number of triple interactions after inhibiting transcription. The observed megadomain triple interactions are compared to a random shuffled control set of interactions.

(D) Histogram of 10,000 random shuffle triple interactions between triptolide treated versus DMSO treated TC-797 cells. *P*-value was determined by comparing the observed ratio to the distribution of shuffled ratios using a random permutation test indicating that the

(E) Percent of inter-chromosomal Hi-C contacts to megadomains in TC-797 cells treated with DMSO shows megadomains that strongly interact with megadomains on other chromosomes coincide with very positive subcompartment scores for subcompartment M (gray shading). Inter-chromosomal Hi-C contacts to megadomains at these loci is retained after inhibition of transcription with triptolide. Purple bars indicate subcompartment M intervals in DMSO treated cells.